LANGMUIR

pubs.acs.org/Langmuir Article

Adsorption of Polar Species at Crude Oil−Water Interfaces: the Chemoelastic Behavior

Ahmed M. Saad, Stefano Aime, Sharath Chandra Mahavadi, Yi-Qiao Song, Maxim P. Yutkin, David Weitz, and Tadeusz W. Patzek*

Cite This: *Langmuir* 2022, 38, 6523−6530 Read Online

ACCESS | Metrics & More | Article Recommendations | Supporting Information

ABSTRACT: We investigate the formation and properties of crude oil/water interfacial films. The time evolution of interfacial tension suggests the presence of short and long timescale processes reflecting the competition between different populations of surface-active molecules. We measure both the time-dependent shear and extensional interfacial rheology moduli. Late-time interface rheology is dominated by elasticity, which results in visible wrinkles on the crude oil drop surface upon interface disturbance. We also find that the chemical composition of the interfacial films is affected by the composition of the aqueous phase that it has contacted. For example, sulfate ions promote films enriched with carboxylic groups and condensed aromatics. Finally, we perform solution exchange experiments and monitor the late-time film composition upon the exchange. We detect the film composition change upon replacing chloride solutions with sulfate-enriched ones. To the best of our knowledge, we are the first to report the composition alteration of aged crude oil films. This finding might foreshadow an essential crude oil recovery mechanism.

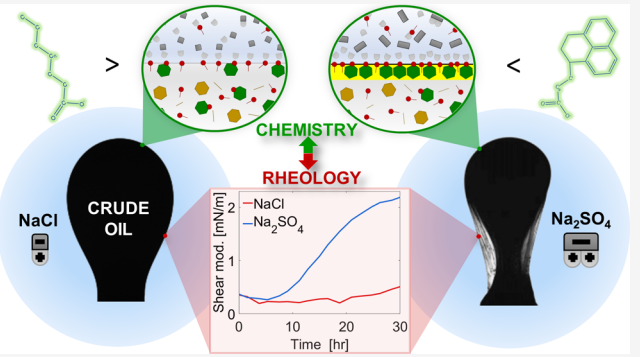

INTRODUCTION

Multicomponent fluids exhibit rich and complex interfacial properties, dictated by each component's mobility and chemical nature. Relating the mechanical properties of complex interfaces to the composition of the bulk materials is vital for many applications, from chemical engineering and food science to biology and medicine.[1] In particular, the interfacial properties of crude oil have received significant attention over the past decades because of their relevance to oil recovery, transport, and processing.[2−4] For example, most oil extraction processes are based on injecting water-based liquids, called brines, into the porous oil reservoir. The efficiency of this process, known as waterflooding, is generally understood as an interplay between viscous and interfacial forces, and it has been shown that it can be enhanced by tuning the chemical composition of the brine, for example, by reducing its salinity or by selectively increasing the concentration of certain divalent ionic species.[5−9] However, despite intense research in this field, the underlying mechanisms that lead to improved oil recovery are still debated.[10−21] Moreover, the complex rheology of the interfacial films dictates the stability of oil/water emulsions, with implications in oil transport, processing, and final quality.[22,23]

For these reasons, adsorption of surface-active moieties at the crude oil-water interface has been extensively studied in the past decades. However, the vast majority of these studies focus only on the measurement of interfacial tension, γ, while the mechanical properties of crude oil−water interfaces may be more complex and require a thorough rheological characterization.[24,25] Interfacial rheology experiments have highlighted, for instance, that many elementary processes, from drop coalescence to snap-off inside rock pores, are often strongly affected by the elasticity of the interfacial film.[13,26,27] Nevertheless, such experiments remain scarce, and their interpretation is controversial due to the lack of a clear connection between the mechanical properties observed in experiments and the underlying physicochemical processes.

In this paper, we investigate the evolution of the interface between crude oil and solutions of different chemical compositions by measuring the interfacial tension as well as the complex shear and extensional viscoelastic moduli of the interface. We find that the formation of interfacial films is nontrivially affected by the chemical composition of the water phase. Furthermore, we analyze the functional groups contributing to the formation of the films using Fourier

Received: January 8, 2022
Revised: April 13, 2022
Published: May 17, 2022

https://doi.org/10.1021/acs.langmuir.2c00058
Langmuir 2022, 38, 6523−6530

transform infrared (FTIR) spectroscopy. We show that the ionic species present in the aqueous phase impact not only the rheology of the interfacial films but also their chemical composition. Our study indicates that, among all molecular species in crude oil, polar aromatic molecules are critical for the formation of viscoelastic interfacial films and that sulfate salts are particularly efficient in promoting their adsorption at the interface, thereby producing more elastic films. Moreover, we show preliminary evidence that this adsorption process is partially reversible and that the properties of fully developed interfacial films can be tuned by changing the composition of the aqueous phase. These results set the basis for a deeper understanding of the chemical origin of the interfacial rheology of complex crude oil systems.

MATERIALS AND METHODS

Chemicals. Deionized (DI) water was obtained from a Milli-Q water purification system (Synergy, EMD Millipore Corporation), which produces type I water with a resistivity greater than 18.2 MΩ cm at 25° C and total organic content less than 10 ppb. The salt used is ACS reagent, ≥99.0%, from Fisher Scientific. Toluene (99.9%, Fisher Scientific) for crude oil dilution was used as received. Crude oil was received from Schlumberger. Its saturate, aromatic, resin, and asphaltene (SARA) composition was obtained using the IP-143 method[28] and is presented in Table 1 along with other physical and chemical properties relevant for this study. In most of our experiments, we used a 3% w/w crude oil solution in toluene. The dilution reduces crude oil viscosity, eases the handling, and allows working with a limited amount of the available sample. To promote dilution, the two fluids were mixed using a vortex mixer for 1 min.

Table 1. SARA Composition and Physical Properties of Crude Oil

property	crude oil
saturates [wt %]	38.3
aromatics [wt %]	19.8
resins [wt %]	36.6
asphaltene [wt %]	3.97
total acid number [mg KOH/g]	1.19
density @ 25 C° [g/cm^3]	0.955
viscosity [cP]	1290

Interfacial Rheology. We probe the mechanical properties of the interfacial films using both dilational and shear interfacial rheology. Dilational rheology experiments are performed using an optical tensiometer (Biolin Theta Flex TF300 with PD200 oscillating drop module), where an oil droplet is formed at the tip of a 14 gauge inverted needle inside a 30 mL glass cell filled with the aqueous phase. The droplet volume is periodically modulated with a prescribed amplitude and frequency using an automated syringe pump and a piezo pump. A camera records the droplet shape, which is then analyzed to obtain the time-dependent surface area, $A(t)$, dynamic interfacial tension, $\gamma(t)$, and complex interfacial modulus, E^{**}.[29] A strain amplitude of 0.5% and a frequency of 0.1 Hz were used for all dilational rheology experiments. The first measurement starts 5 s after complete droplet inflation to the desired volume.

Shear rheology experiments are performed using a Discovery Hybrid Rheometer from TA Instruments, equipped with a Double Wall Ring interfacial geometry. A commercial double wall ring cell was customized with homemade components, as shown in the Supporting Information (Figure S1), to reduce the evaporation of volatile components in crude oil and toluene during experiments lasting several days.[30] In addition, our shear rheology setup allows us to wash the bulk oil phase at the end of the experiment using pure toluene without disrupting the interfacial film, thereby enabling the collection of the interfacial material. All shear rheology experiments were performed at 0.1% strain amplitude and 1 Hz frequency. The choice of amplitude and frequency for both shear and dilational rheology is further discussed in the Supporting Information (Figures S2, S3).

FTIR Spectroscopy. To examine the chemical composition of the interfacial films, we recorded the FTIR spectra of the interfacial films collected from the oil−water interfaces. The interfacial material was collected using a procedure described in detail elsewhere.[31,32] Here, we provide the key details for the reader and a schematic of the process (see Supporting Information, Figure S9). The interfacial material was formed by layering a crude oil−toluene mixture (3% vol) on top of an aqueous solution in a wide glass dish to maximize the contact area. After the layering, the organic material in the crude oil−toluene mixture was allowed to adsorb at the toluene−water interface for 24 h. Afterward, the toluene phase was removed by repeated dilution, followed by decantation. Eventually, pure toluene on top of the interfacial material was allowed to evaporate, and the interfacial material was collected from the water−air interface by a Teflon spatula. Then, the collected material was dissolved in dichloromethane. The dichloromethane solution was deposited dropwise on the ATR crystal of an FTIR spectrometer. After the evaporation of dichloromethane, FTIR spectra were recorded using a Varian 670-IR FTIR spectrometer in the attenuated total reflectance (ATR) mode with MIRacle ATR accessory from PIKE Technologies. All measurements were performed under a nitrogen blanket.

RESULTS AND DISCUSSION

Adsorption Kinetics. We study the adsorption kinetics at the crude oil−water interface by monitoring the time evolution of the surface tension, $\gamma(t)$, using a pendant drop apparatus. When the interface is formed against a deionized water phase, we find that $\gamma(t)$ starts from a short-time value γ_0 of about 28 mN/m and decays logarithmically in time, without approaching a well-defined steady state within the 24 h time window probed by experiments, as shown by the black data points in Figure 1. This indicates that the adsorption and equilibration of surface-active molecules at the interface is an extremely slow process, characterized by timescales much beyond those set by the mobility of molecules in the bulk phases. Such slow dynamics suggests that this regime is dominated by molecular interactions, which hinder molecular migration and reorganization at the interface.[33,34]

As salts are added to the aqueous phase; however, $\gamma(t)$ develops a very unusual, nonmonotonic decay: at the earliest times experimentally accessible, we find that it starts from a relatively low value γ_0, then starts rising, and subsequently joins the logarithmic decrease, typical of DI water−oil interfaces. We observe that this first nonmonotonic transient regime depends on the water chemistry, with different salts associated with different γ_0, as shown in Figure 1a. To confirm this hypothesis, we study the impact of salt concentration, and we find that, as expected, larger salt concentrations are associated with a lower γ_0, as shown in Figure 1b. Such nonmonotonic behavior of $\gamma(t)$ is rather unusual, as it implies that the total surface energy spontaneously undergoes a transient growth. Our data show that all $\gamma(t)$ curves start raising at the same time, joining the DI water curve at time $t_I \approx 10$ min, quite independent of salt chemistry and concentration. Thus, because the timescale associated with this growth is independent of the chemical composition of the water phase, we investigate the role of the oil phase by fixing the water phase to 0.1 M NaCl solution and changing the concentration of crude oil in toluene, c_c. As c_c is decreased, we find that the transient increase in $\gamma(t)$ becomes slightly slower and less pronounced, and it disappears completely for the lowest value of c_c tested, as shown in

https://doi.org/10.1021/acs.langmuir.2c00058
Langmuir 2022, 38, 6523−6530

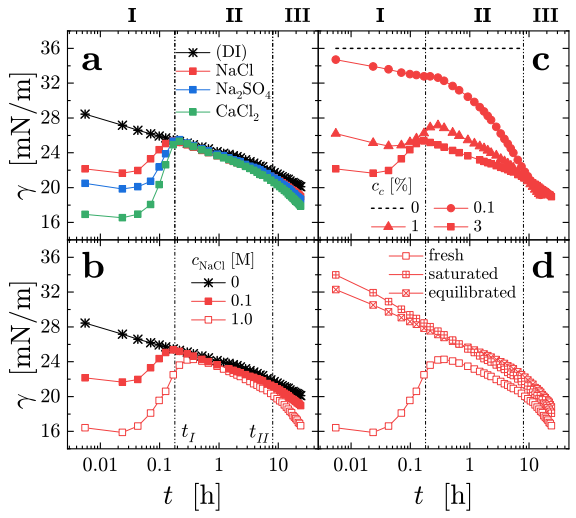

Figure 1. Adsorption kinetics. Interfacial tension, γ, plotted against time, t, since droplet formation, varying (a) salt chemistry, at fixed salt concentration (0.1 M) and crude oil concentration (3%); (b) salt concentration, c_{NaCl}, for fixed salt chemistry (NaCl) and crude oil concentration (3%); (c) crude oil concentration, c_c (w/w, in toluene), for fixed aqueous phase (0.1 M NaCl); (d) effect of equilibration protocol, for fixed aqueous phase (1 M NaCl) and oil concentration (3%). The first measurement is recorded 5 s after the initial droplet inflation to the desired size. The top labels mark the three steps of film formation [(I) $t < 0.18$ h, early stage; (II) 0.18 h $< t <$ 8 h, film formation; (III) $t >$ 8 h, network aging].

Figure 1c. By contrast, the decay of $\gamma(t)$ for $t > t_I$ becomes much faster for lower c_c. A similar early-time nonmonotonic behavior has been reported in the literature for crude oil,[35−37] but to the best of our knowledge, no detailed explanation has been proposed so far.

To understand this behavior, we consider the complex, multicomponent nature of crude oil, composed of a wide spectrum of chemical species of different sizes, polarity, and mobility. Among the molecules containing polar groups, thus susceptible to adsorption at the oil−water interface, we schematically isolate the contribution of two families of molecules: (A) small molecules, with the polar head connected to a relatively small hydrophobic tail and (B) large molecules, with the polar groups bound to a larger hydrophobic body. Being characterized by larger mobility, (A) molecules adsorb faster at the interface, dictating the short-time value of γ_0. The presence of ionic species in the water phase favors the deprotonation of the acid groups of the adsorbed molecules, thereby increasing the energy gain for adsorption. This results in faster adsorption kinetics and thus a faster drop in $\gamma(t)$ at very early times before the first experimental point is measured. The dependence of γ_0 on the salt chemistry then stems from the effect of each salt species on the adsorption energy, with the divalent cation (Ca^{2+}) associated to the largest decrease in γ_0, indicative of a larger energy gain, followed by Na_2SO_4, which provides twice as many monovalent cations (Na^+) as NaCl at equal molarity. However, because of their comparatively short hydrophobic tail, (A) molecules may be partially soluble in the water phase, depending on its salinity.[38−40] Thus, at later times, (A) molecules adsorbed at the interface may partition in the water phase, leading to an increase in $\gamma(t)$, leaving some room for the adsorption of (B) molecules. This second process is much slower, as the mobility of (B) molecules is further hindered by their size and intermolecular interactions.[33,34,41,42]

To test this model, we measure $\gamma(t)$ in the oil−water systems that have previously been in contact, such that the partitioning of (A) molecules has occurred prior to the droplet formation. To this end, we presaturate the aqueous phase by multiple extractions of the water-soluble components. Saturation is obtained by keeping the water and oil phases in contact for 15 min with intermittent shaking and by subsequently replacing the oil phase with a fresh sample. This process is repeated five times, after which the bulk phases are extracted. We investigate another condition that we refer to as equilibrated, where the two fluids are kept in contact and shaken for 15 min only. Eventually, we inflate a droplet of either saturated or equilibrated crude oil sample surrounded by the saturated water phase. The resulting $\gamma(t)$ exhibits in both cases a monotonic logarithmic decrease, as shown in Figure 1d, confirming that the transient growth in $\gamma(t)$ is indeed related to the partitioning of (A) molecules into the water phase.

At the latest stages of the experiments, we find that if the salinity of the water phase is large enough, $\gamma(t)$ deviates once again from the logarithmic decay found for DI water and exhibits a faster decay. This suggests the onset of an even slower process around $t_{II} \approx 8$ h: we anticipate that it corresponds to the formation of an elastic interfacial skin, as we shall see in the next section.

Rheology of the Interfacial Films. As we deflate the droplet by withdrawing the syringe after the development of $\gamma(t)$ for 24 h, we find that the droplet does not shrink homogeneously: instead, its surface develops wrinkles, as shown in Figure 2a. This indicates that molecules that adsorb at the interface interact with each other to form a solid skin.[43] To characterize the mechanical properties of this skin, we perform time-resolved dilational rheology experiments on the droplet. To this end, we use a piezo pump to impose a small periodic perturbation at frequency $\omega = 0.1$ Hz to the volume of the droplet, and we record its subsequent change in shape. This enables the measurement of the complex dilational modulus $E^{s*}(\omega)$ of the interface, describing the mechanical stress associated with its periodic extensional deformation.[29] We find that the mechanical response is largely dominated by the real part of E^{s*}, which is the elastic dilational modulus, $E^{s\prime}$, describing the stress component in phase with the applied deformation (see Supporting Information, Figure S4). Furthermore, we find that $E^{s\prime}$ grows logarithmically in time for all samples tested, as shown by the full symbols in Figure 2b.

The remarkable overlap of all $E^{s\prime}(t)$, together with their logarithmic time dependence, resembles that of $\gamma(t)$ in the intermediate regime of film formation, as shown in Figure 1a. The analogy between the two quantities suggests that here $E^{s\prime}$ is dominated by Gibbs elasticity, which describes the dependence of γ on the surface coverage, Γ. Indeed, the periodic modulation in the surface area applied to measure $E^{s\prime}$ entails a periodic modulation of surface coverage, which reflects in the time-dependent surface tension that effectively contributes to the measured elastic modulus. This contribution is called the Gibbs modulus,[44] $E_G = -\mathrm{d}\gamma/\mathrm{d}\ln\Gamma$, and provides information on the equation of state $\gamma(\Gamma)$. An analytic solution for $\gamma(\Gamma)$ can be derived by recognizing that $E^{s\prime}(t)$ is proportional to the interfacial tension decay, $\delta\gamma(t) = \gamma(t) - \gamma_r$, with γ_r being a reference tension representative of the naked interface. Under the working hypothesis that $E_G \approx E^{s\prime} =$

https://doi.org/10.1021/acs.langmuir.2c00058
Langmuir 2022, 38, 6523−6530

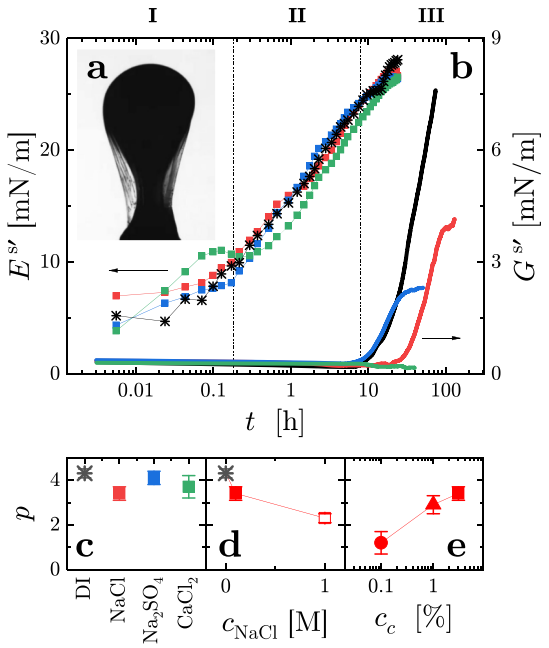

Figure 2. Rheology of interfacial films. (a) Snapshot of a wrinkled droplet surface produced as the droplet is deflated after long-time skin formation (24 h) in contact with DI water. (b) Extensional elastic modulus ($E^{s\prime}$, squares, left axis) and shear elastic modulus ($G^{s\prime}$, solid lines, right axis) as a function of time for varying salt chemistry, at fixed salt concentration (0.1 M) and crude oil concentration (3%). Colors indicate salt chemistry, as in Figure 1a. (c–e) Equation-of-state exponent, p, for different salt species (c), salt concentration (d), and crude oil concentration (e).

$-p\delta\gamma$, with p a sample-dependent constant prefactor, we obtain a differential equation in $\delta\gamma(\Gamma)$: d ln $\delta\gamma$/d ln Γ = p. The solution of this equation is a power-law dependence on surface coverage: $E^{s\prime} \propto \delta\gamma \propto \Gamma^p$.

To extract the characteristic exponent, p, from our experimental data, we fit both $E^{s\prime}(t)$ and $\gamma(t)$ for $t_I < t < t_{II}$ to the logarithmic growth and decay, respectively. The fits yield a characteristic time, τ, such that $E^{s\prime}_{fit}(\tau) = 0$, and a reference surface tension, $\gamma_r = \gamma_{fit}(\tau)$. From this, we calculate $\delta\gamma(t)$, and we extract $p = \langle -E^{s\prime}/\delta\gamma \rangle_{t_I<t<t_{II}}$, where $\langle \cdots \rangle_{t_I<t<t_{II}}$ denotes averaging over all data points in the regime where logarithmic dependence is observed (see Supporting Information, Figure S5). By repeating this analysis on all measured samples, we find that p depends weakly on salt chemistry and decreases with both increasing salt concentration and decreasing oil concentration, as shown in Figure 2c–e. This result highlights the physical meaning of p: a smaller p reflects a weaker dependence of $E^{s\prime}$ and γ on surface coverage. Thus, in analogy to 3D bulk systems,[45] we interpret p as a measurement of the softness of the interface, smaller p representing softer interfaces. This softness may be attributed to intermolecular interactions, which promote clustering at the interface, inhibiting the molecular restructuring required to increase the surface coverage further. Indeed, from the logarithmic decay of $\delta\gamma(t)$, we find that $\Gamma(t) \propto [\ln(t/\tau)]^{1/p}$, implying that larger p entails a slower evolution of $\Gamma(t)$. In these terms, the increase of p with c_c, shown in Figure 2e, suggests that larger oil concentration yields faster and more disordered crowding at the interface, whereas the decrease of p with c_{NaCl}, shown in Figure 2d, suggests that larger salt concentrations favor molecular ordering, as found in some surfactant systems.[46]

Thus, this notion of interfacial softness efficiently accounts for our experimental results. In addition, the weaker dependence of p on salt chemistry, shown in Figure 2c, suggests that intermolecular interactions depend on salt chemistry, with weaker interactions in the case of chloride salt films; this is key to understanding the onset of complex interfacial rheology.

In fact, while the Gibbs elasticity is useful to derive the equation of state $\gamma(\Gamma)$, it does not inform on the deviatoric surface stresses leading to wrinkles and crumpling of the droplet skin.[47,48] Indeed, we observe that the oil droplet retracts smoothly if the liquid is withdrawn before t_{II}, whereas it develops wrinkles, shown in Figure 2a, when oil is withdrawn during the latest stage of film formation, where $E^{s\prime}$ is no longer proportional to $\delta\gamma$. To study the onset of these deviatoric surface stresses, we use shear interfacial rheology, which probes the complex shear modulus of the interface, $G^{s*}(\omega)$. Because it describes the mechanics of the interface at a constant surface area, $G^{s*}(\omega)$ is completely insensitive to surface tension. We find that its absolute value is below the sensitivity limit of the instrument (about 0.1 mN/m) throughout the first two phases of film formation and only becomes measurable during the third phase. In this phase, we find that $G^{s*}(\omega)$ is dominated by its real part, $G^{s\prime}$, which is the shear storage modulus, and is shown as thick solid lines in Figure 2b. The shear modulus shows a strong dependence on the aqueous phase chemistry with DI water and Na_2SO_4 films, developing a measurable $G^{s\prime}$ first. The chloride salt films show a delayed onset of shear elasticity, with no measurable modulus in the case of the $CaCl_2$ film during the timescale of the experiment. This is in agreement with the lower p observed in Figure 2, and it is in contrast to the early-time evolution of $\gamma(t)$, for $t < t_I$, which was rather dictated by the amount and valency of the cations, Na^+ and Ca^{2+}, with little or no impact of the anions, Cl^- and SO_4^{2-}. This contrast further confirms that the initial adsorption and the formation of the interfacial skin at longer times are independent processes. A deeper understanding of these mechanisms may help in rationalizing the results reported in the literature about wettability alteration and efficiency of oil recovery, for which no robust explanation has been proposed.[10,49]

Chemical Composition of the Interfacial Films. To understand the origin of this complex rheology and the differences between interfacial films produced with different salts, we analyzed the chemical composition of the interfacial material using FTIR. To highlight the specificity of adsorbed molecules, we first compare the composition of interfacial materials with that of bulk crude oil, shown as a dashed gray line in Figure 3a. We find that for bulk crude oil, the spectrum is dominated by a pair of pronounced peaks around 1400 cm^{-1}, coming from methyl and methylene groups, with a shallower peak at 1600 cm^{-1}, indicating the presence of aromatic C=C bonds. There is no significant signature of any other functional groups, in line with the composition reported in Table 1, dominated by saturates and aromatics. By contrast, interfacial materials exhibit richer spectra, shown as solid lines in Figure 3a, with different colors reflecting different aqueous phase chemistries. With respect to bulk crude oil, they all exhibit an additional peak around 1730 cm^{-1}, which corresponds to the stretching of the C=O bond of carbonyl groups and indicates that interfacial materials are enriched with polar carboxylic acid groups.[31] In addition, interfacial materials have enhanced spectra in the so-called fingerprint region, between 650 and 1200 cm^{-1}. In particular, we focus on the

https://doi.org/10.1021/acs.langmuir.2c00058
Langmuir 2022, 38, 6523–6530

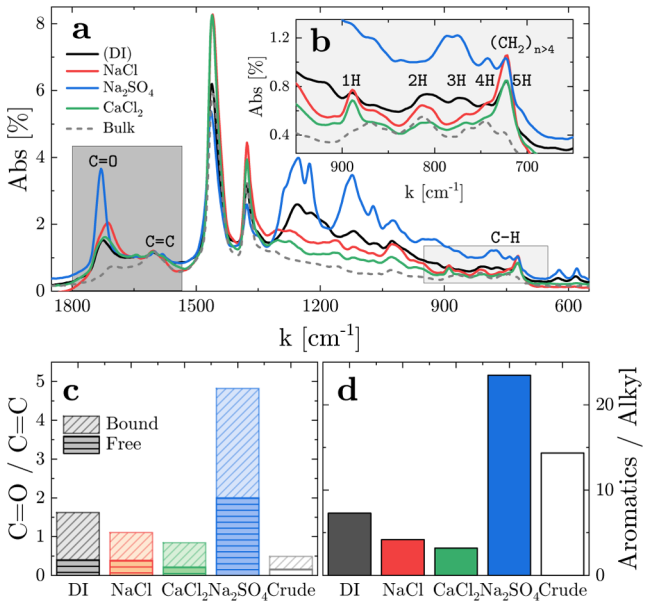

Figure 3. Chemical composition of interfacial films. (a) FTIR spectra of interfacial films and bulk crude oil between 550 and 1850 cm^{-1}, highlighting the acid region (1550−1800 cm^{-1}) and the fingerprint region (650−750 cm^{-1}). (b) Fingerprint region of the spectra showing the peaks corresponding to different substitutions of aromatic rings (number of adjacent hydrogen atoms) as well as the peak corresponding to the alkyl chain with more than four carbons. (c) Concentration of carboxylic acid group relative to the C═C peak (1600 cm^{-1}), obtained as the integral areas of the deconvoluted peaks. (d) Concentration of aromatic moieties relative to the $(CH_2)_{n>4}$ peak (727 cm^{-1}) of long alkyl chains.

range between 650 and 950 cm^{-1}, which is expanded in Figure 3b, highlighting the degree of condensation and substitutions on the aromatic groups. In this region, we identify five peaks, marked by labels 1H, ..., 5H, which correspond to aromatic rings with one to five neighboring hydrogen atoms, as schematically illustrated in Supporting Information, Figure S11. In addition, our spectra exhibit a pronounced peak at 727 cm^{-1}, which indicates the presence of long aliphatic chains $(CH_2)_{n>4}$ almost invisible in bulk crude oil. Despite these common features, the FTIR spectra of interfacial materials produced against solutions with different chemical compositions exhibit quantitative differences, suggesting that the aqueous phase chemistry does impact the film composition. In particular, we find that NaCl and $CaCl_2$ produce similar spectra (red and green lines in Figure 3), whereas Na_2SO_4 (blue line) forms interfacial films with a quite different chemical composition, more enriched in carboxylic acids and highly condensed aromatics, as shown by the enhanced C═O peak and fingerprint peaks, respectively. This suggests that the chemical nature of the counterions, Cl^- and SO_4^{2-}, has a stronger impact on the properties of the interfacial materials than the valency of cations, in agreement with the rheology data shown in Figure 2.

This analogy further motivates the search for the chemical origin of the mechanical properties of our interfacial films. To this end, we estimate the relative concentrations of different functional groups through deconvolution by fitting the FTIR spectra to a sum of Gaussian curves. We then estimate the relative amount of each functional group by summing over the areas of all curves within the expected range of wavenumbers. To properly account for different sample volumes and for the absorbance coefficients of different functional groups, we normalize our results by the area of the C═C peak, which we take as a reference signal. Details of the fitting protocol and results are given in Supporting Information, Section S6. We find that the relative amount of carboxylic acid groups is several times larger in films formed against Na_2SO_4 than in the others, as shown in Figure 3c. In addition, we observe that the detailed shape and position of the C═O peak differs from sample to sample. We interpret this as a result of the heterogeneous chemical environment surrounding the C═O bond, whose absorption peak shifts toward smaller wavenumbers when the carbonyl group is either in conjugation with a double bond or an aromatic group or H-bonded with another molecule.[50] Therefore, we classify the contribution of the carbonyl group as bound, or conjugated, for peak positions below 1725 cm^{-1}, and free, or nonconjugated ones, for positions above it,[50] shown as diagonally and horizontally striped bar plots in Figure 3c, respectively. The results highlight that free carbonyl groups are particularly more abundant in films formed against solutions rich in sulfate salts, suggesting that in these films, a larger fraction of molecules have the carbonyl group connected to a bulkier tail which could prevent H bonding due to steric hindrance.

To test this hypothesis, we apply a similar analysis to the fingerprint region, where we integrate all aromatic peaks to estimate the total concentration of aromatics, and we normalize it by the area of the $(CH_2)_{n>4}$ peak representing the amount of long alkyl chains. We find that films formed in the presence of Na_2SO_4 exhibit the largest amount of aromatic groups, followed by DI water and chloride salts, as shown in Figure 3d. The strong correlation between aromatic and free acid contents suggests that the two signals come from the same polar aromatic molecules adsorbed at the interface. The polar nature of these molecules promotes their stability at the interface, while their aromatic structure promotes intermolecular interactions through $\pi-\pi$ stacking, leading to the formation of a complex viscoelastic interfacial skin.

Adsorption Reversibility. The FTIR spectra highlight that the chemical composition of interfacial films depends on that of the water phase, which then dictates the mechanical properties of the oil−water interface. This result suggests that it may be possible to alter the composition and rheology of the interfacial films through the aqueous phase chemistry, provided that the adsorption process is at least partially reversible. This is an important insight with implications for oil recovery. Indeed, the change in the film composition could alter its physical properties that in turn could result in more efficient brine imbibition, oil expulsion, and thus higher incremental oil recovery.

To test the reversibility of molecular adsorption, we first prepare an interfacial film against 0.1 M NaCl, let it develop over 3 days, and gently replace the water phase with 0.1 M Na_2SO_4 solution. In the proximity of the interface, this salt switch process is slow and driven by diffusion, such that the interface is only affected by the change in solution composition and not by the flow applied to replace the water phase. More details are given in Supporting Information, Section S7. After 3 additional days of equilibration, we collect the interfacial material and examine its chemical composition through FTIR analysis. We find that the change in aqueous phase chemistry entails a change in the composition of the interfacial film, whose spectrum departs from that of films formed against NaCl solution and develops features typical of Na_2SO_4 brine,

https://doi.org/10.1021/acs.langmuir.2c00058
Langmuir 2022, 38, 6523−6530

namely, a larger aromatic content relative to the long alkyl chains and a larger amount of free carboxyl groups relative to the bound ones, as shown by the shift of the C═O peak in Figure 4a, and quantified in Figure 4b. The deconvolution

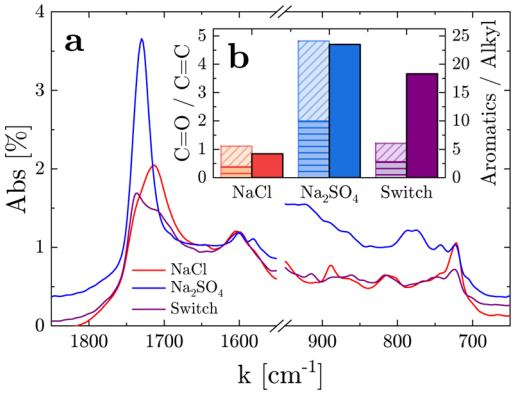

Figure 4. Adsorption reversibility. The switch film (NaCl ⇒ Na_2SO_4) is compared to the ones formed independently with NaCl and Na_2SO_4 salt (all of 0.1 M concentration), showing the acid region of the FTIR spectra (1500−1900 cm^{-1}) and the fingerprint region (650−950 cm^{-1}). (b) Quantification of relative concentrations of carboxylic acids (dashed diagonal: bound; dashed horizontal: free) and aromatics (solid bars) using the areas of deconvoluted peaks. The salt switch film appears to be a combination of individual salt films.

details are presented in Supporting Information, Figure S16. This result indicates that the adsorption process is indeed partially reversible and that the composition of a fully developed interfacial film can be altered by changing the aqueous phase chemistry. More experiments are required to quantitatively assess the dynamics and steady state of interfacial film after the solution switch and its impact on interfacial rheology. This observation can help in understanding the reported preferential change in wettability in the presence of sulfate salts.[10]

CONCLUSIONS

In this work, we have investigated the formation of interfacial films between crude oil and aqueous electrolyte solutions, using a combination of experimental techniques allowing us to probe the time evolution of interfacial tension, γ, the shear, and extensional elastic moduli, $G^{s\prime}$ and $E^{s\prime}$, and the chemical composition of interfacial films aged for 24 h. We found that the complex kinetics characterizing film formation can be simplified by considering the competition between two classes of surface-active molecules. This competition gives rise to three distinct phases of film formation. In the earliest stages, smaller polar molecules adsorb quickly at the interface, causing an early drop in γ, which depends on the solution composition, namely on the concentration and valence of the cations in the aqueous phase. At later times, these small molecules partition to the aqueous phase and are gradually replaced at the interface by larger molecules, with polar groups and bulk aromatic systems. These replacements cause a transient, nonmonotonic evolution of γ, followed by a logarithmic evolution of both γ and $E^{s\prime}$, independent of the aqueous phase composition. The mechanical properties of the interface in this regime are dominated by high elasticity ($E^{s\prime}$).

The latest stage of film formation is characterized by a deviation from the simple, logarithmic evolution of γ and $E^{s\prime}$ and by the onset of a measurable shear elastic modulus, $G^{s\prime}$. This onset reveals that the adsorbed molecules interact with each other, forming a rigid network with solid-like rheological properties. We find that the onset of shear elasticity is enhanced in films formed against sulfate-enriched solutions.

The chemical analysis of the fully developed (aged for 24 h) interfacial films revealed that films adsorbed on aqueous solutions of Na_2SO_4 contain a notably larger amount of polar aromatic compounds. We suggest that these compounds play a pivotal role in the formation of interfacial elastic films: polar groups help stabilize the adsorbed molecules at the interface, while the aromatic molecular body promotes intermolecular $\pi-\pi$ interactions favoring the development of an interconnected molecular network at the interface.

Although the adsorption of asphaltenes at crude oil interfaces is thought to be irreversible, we were able to desorb some of the components of the developed interfacial network. The observed partial reversibility of the molecular adsorption upon switching from chloride- to sulfate-rich solutions confirms the possibility of tuning the physicochemical properties of the interfacial films. Further studies relating the chemical composition of films developed with different brines in contact with reservoir rock minerals and their corresponding surface contact angles would be needed to provide practical guidelines for oil field operations regarding wettability alteration to maximize oil recovery.

ASSOCIATED CONTENT

Supporting Information

The Supporting Information is available free of charge at https://pubs.acs.org/doi/10.1021/acs.langmuir.2c00058.

More details of the shear and dilational rheology experiments, interfacial surface coverage calculations for diluted crude oil, more experimental details of sample preparation and FTIR chemical analysis, detailed results of the FTIR spectra deconvolution, and salt replacement experiments (PDF)

AUTHOR INFORMATION

Corresponding Author

Tadeusz W. Patzek − *Ali I. Al-Naimi Petroleum Engineering Research Center, King Abdullah University of Science and Technology, Thuwal 23955-6900, Saudi Arabia;* orcid.org/0000-0002-9389-7579; Email: tadeusz.patzek@kaust.edu.sa

Authors

Ahmed M. Saad − *Ali I. Al-Naimi Petroleum Engineering Research Center, King Abdullah University of Science and Technology, Thuwal 23955-6900, Saudi Arabia;* orcid.org/0000-0003-4078-5917

Stefano Aime − *John A. Paulson School of Engineering and Applied Sciences, Harvard University, Cambridge, Massachusetts 02138, United States; Molecular, Macromolecular Chemistry, and Materials, ESPCI Paris, CNRS, PSL University, Paris 75005, France*

Sharath Chandra Mahavadi − *Schlumberger-Doll Research, Cambridge, Massachusetts 02139, United States;* orcid.org/0000-0001-5171-5207

Yi-Qiao Song − *Schlumberger-Doll Research, Cambridge, Massachusetts 02139, United States; Athinoula A. Martinos Center for Biomedical Imaging, Department of Radiology,*

https://doi.org/10.1021/acs.langmuir.2c00058
Langmuir 2022, 38, 6523−6530

Massachusetts General Hospital, Charlestown, Massachusetts 02129, United States

Maxim P. Yutkin − *Ali I. Al-Naimi Petroleum Engineering Research Center, King Abdullah University of Science and Technology, Thuwal 23955-6900, Saudi Arabia*

David Weitz − *John A. Paulson School of Engineering and Applied Sciences and Department of Physics, Harvard University, Cambridge, Massachusetts 02138, United States;* orcid.org/0000-0001-6678-5208

Complete contact information is available at: https://pubs.acs.org/10.1021/acs.langmuir.2c00058

Notes

The authors declare no competing financial interest.

■ ACKNOWLEDGMENTS

The research reported in this publication has been supported by KAUST through baseline research funding to Prof. Patzek and by CUPB (CUP grant no. B13010), NSF grant no. DMR-1708729, and through the Harvard University Materials Research Science and Engineering Center (NSF grants nos. DMR-1420570 and DMR-2011754). Crude oil samples were provided by Schlumberger-Doll Research. The authors thank all five anonymous reviewers for their thoughtful detailed requests and comments that greatly improved this paper.

■ REFERENCES

(1) Masschaele, K.; Vandebril, S.; Vermant, J.; Madivala, B. Interfacial rheology. *Rheology*; *CRC Press*, 2010; Vol. *I*, p 414.

(2) Strassner, J. E.; et al. Effect of pH on interfacial films and stability of crude oil-water emulsions. *J. Pet. Technol.* **1968**, *20*, 303−312.

(3) Reisberg, J.; Doscher, T. M. Interfacial phenomena in crude oil-water systems. *Prod. Mon.* **1956**, *21*, 43−50.

(4) Freer, E. M.; Radke, C. J. Relaxation of asphaltenes at the toluene/water interface: diffusion exchange and surface rearrangement. *J. Adhes.* **2004**, *80*, 481−496.

(5) Patzek, T.; Saad, A.; Hassan, A. Multimodal Carbonates: Distribution of Oil Saturation in the Microporous Regions of Arab Formations. *Energies* **2022**, *15*, 1243.

(6) Reiter, P. K. A water-sensitive sandstone flood using low salinity water. Ph.D. Thesis, University of Oklahoma, 1961.

(7) Jadhunandan, P.; Morrow, N. *Spontaneous imbibition of water by crude oil/brine/rock systems*; United States, 1991; p 15. In Situ.

(8) Yildiz, H. O.; Morrow, N. R. Effect of brine composition on recovery of Moutray crude oil by waterflooding. *J. Pet. Sci. Eng.* **1996**, *14*, 159−168.

(9) Tang, G.-Q.; Morrow, N. R. Influence of brine composition and fines migration on crude oil/brine/rock interactions and oil recovery. *J. Pet. Sci. Eng.* **1999**, *24*, 99−111.

(10) Strand, S.; Høgnesen, E. J.; Austad, T. Wettability alteration of carbonates—Effects of potential determining ions (Ca2+ and SO42-) and temperature. *Colloids Surf., A* **2006**, *275*, 1−10.

(11) Zahid, A.; Stenby, E. H.; Shapiro, A. A., et al. Improved oil recovery in chalk: wettability alteration or something else? *SPE Europec/eage Annual Conference and Exhibition*, 2010.

(12) Fathi, S. J.; Austad, T.; Strand, S. Water-based enhanced oil recovery (EOR) by "smart water": Optimal ionic composition for EOR in carbonates. *Energy Fuels* **2011**, *25*, 5173−5179.

(13) Alvarado, V.; Moradi Bidhendi, M.; Garcia-Olvera, G.; Morin, B.; Oakey, J. S., et al. Interfacial visco-elasticity of crude oil-brine: An alternative EOR mechanism in smart waterflooding. *SPE Improved Oil Recovery Symposium*, 2014.

(14) Austad, T.; Shariatpanahi, S. F.; Strand, S.; Aksulu, H.; Puntervold, T. Low salinity EOR effects in limestone reservoir cores containing anhydrite: a discussion of the chemical mechanism. *Energy Fuels* **2015**, *29*, 6903−6911.

(15) Derkani, M.; Fletcher, A.; Abdallah, W.; Sauerer, B.; Anderson, J.; Zhang, Z. Low salinity waterflooding in carbonate reservoirs: review of interfacial mechanisms. *Colloids Interfaces* **2018**, *2*, 20.

(16) Fattahi Mehraban, M.; Farzaneh, S. A.; Sohrabi, M.; Sisson, A. Novel Insights into the Pore-Scale Mechanism of Low Salinity Water Injection and the Improvements on Oil Recovery. *Energy Fuels* **2020**, *34*, 12050−12064.

(17) Kovscek, A. R.; Wong, H.; Radke, C. J. A pore-level scenario for the development of mixed wettability in oil reservoirs. *AIChE J.* **1993**, *39*, 1072−1085.

(18) Yan, J.; Plancher, H.; Morrow, N. R.; et al. Wettability changes induced by adsorption of asphaltenes. *SPE Prod. Facil.* **1997**, *12*, 259−266.

(19) Kaminsky, R.; Radke, C. J. Asphaltenes, water films, and wettability reversal. *SPE J.* **1997**, *2*, 485−493.

(20) Yutkin, M. P.; Mishra, H.; Patzek, T. W.; Lee, J.; Radke, C. J. Bulk and Surface Aqueous Speciation of Calcite: Implications for Low-Salinity Waterflooding of Carbonate Reservoirs. *SPE J.* **2018**, *23*, 084−101.

(21) Yutkin, M.; Radke, C.; Patzek, T. *Chemical Compositions in Modified Salinity Waterflooding of Calcium Carbonate Reservoirs: Experiment*; Transport in Porous Media, 2022; pp 1−24.

(22) Sjöblom, J.; Aske, N.; Harald Auflem, I.; Brandal, Ø.; Erik Havre, T.; Sæther, Ø.; Westvik, A.; Eng Johnsen, E.; Kallevik, H. Our current understanding of water-in-crude oil emulsions.: Recent characterization techniques and high pressure performance. *Adv. Colloid Interface Sci.* **2003**, *100−102*, 399−473.

(23) Lesaint, C.; Glomm, W. R.; Lundgaard, L. E.; Sjöblom, J. Dehydration efficiency of AC electrical fields on water-in-model-oil emulsions. *Colloids Surf., A* **2009**, *352*, 63−69.

(24) Alicke, A.; Simon, S.; Sjöblom, J.; Vermant, J. Assessing the Interfacial Activity of Insoluble Asphaltene Layers: Interfacial Rheology versus Interfacial Tension. *Langmuir* **2020**, *36*, 14942−14959.

(25) Samaniuk, J. R.; Hermans, E.; Verwijlen, T.; Pauchard, V.; Vermant, J. Soft-glassy rheology of asphaltenes at liquid interfaces. *J. Dispersion Sci. Technol.* **2015**, *36*, 1444−1451.

(26) Moradi, M.; Alvarado, V. Influence of aqueous-phase ionic strength and composition on the dynamics of water−crude oil interfacial film formation. *Energy Fuels* **2016**, *30*, 9170−9180.

(27) Bochner de Araujo, S.; Merola, M.; Vlassopoulos, D.; Fuller, G. G. Droplet Coalescence and Spontaneous Emulsification in the Presence of Asphaltene Adsorption. *Langmuir* **2017**, *33*, 10501−10510.

(28) Standard IP 143/90. Asphaltene (Heptane Insolubles) in Petroleum Products. *Standards for Petroleum and Its Products*; Institute of Petroleum: London, 1985.

(29) Ravera, F.; Loglio, G.; Kovalchuk, V. I. Interfacial dilational rheology by oscillating bubble/drop methods. *Curr. Opin. Colloid Interface Sci.* **2010**, *15*, 217−228.

(30) Saad, A. M.; Aime, S.; Mahavadi, S. C.; Song, Y.-Q.; Patzek, T. W.; Weitz, D. Interfacial Viscoelasticity in Crude Oil-Water Systems to Understand Incremental Oil Recovery. *SPE Annual Technical Conference and Exhibition*. 2020.

(31) Andersen, S. I.; Chandra, M. S.; Chen, J.; Zeng, B. Y.; Zou, F.; Mapolelo, M.; Abdallah, W.; Buiting, J. J. Detection and impact of carboxylic acids at the crude oil−water interface. *Energy Fuels* **2016**, *30*, 4475−4485.

(32) Andersen, S. I.; Mahavadi, S. C.; Abdallah, W.; Buiting, J. J. Infrared Spectroscopic Analysis of the Composition of an Oil/Water Interfacial Film. *Energy Fuels* **2017**, *31*, 8959−8966.

(33) Pauchard, V.; Rane, J. P.; Zarkar, S.; Couzis, A.; Banerjee, S. Long-term adsorption kinetics of asphaltenes at the oil−water interface: A random sequential adsorption perspective. *Langmuir* **2014**, *30*, 8381−8390.

(34) Zhang, S.; Zhang, L.; Lu, X.; Shi, C.; Tang, T.; Wang, X.; Huang, Q.; Zeng, H. Adsorption kinetics of asphaltenes at oil/water interface: Effects of concentration and temperature. *Fuel* **2018**, *212*, 387−394.

(35) Nasr-El-Din, H. A.; Taylor, K. C. Dynamic interfacial tension of crude oil/alkali/surfactant systems. *Colloids Surfaces* **1992**, *66*, 23−37.
(36) Jeribi, M.; Almir-Assad, B.; Langevin, D.; Hénaut, I.; Argillier, J. F. Adsorption kinetics of asphaltenes at liquid interfaces. *J. Colloid Interface Sci.* **2002**, *256*, 268−272.
(37) Rane, J. P.; Pauchard, V.; Couzis, A.; Banerjee, S. Interfacial rheology of asphaltenes at oil−water interfaces and interpretation of the equation of state. *Langmuir* **2013**, *29*, 4750−4759.
(38) Whitehouse, B. G. The effects of temperature and salinity on the aqueous solubility of polynuclear aromatic hydrocarbons. *Mar. Chem.* **1984**, *14*, 319−332.
(39) Al-Enezi, G.; Ettouney, H.; El-Dessouky, H.; Fawzi, N. Solubility of sulfur dioxide in seawater. *Ind. Eng. Chem. Res.* **2001**, *40*, 1434−1441.
(40) Bertheussen, A.; Simon, S.; Sjöblom, J. Equilibrium partitioning of naphthenic acids and bases and their consequences on interfacial properties. *Colloids Surf., A* **2017**, *529*, 45−56.
(41) Oliver, J. W. H. Diffusion of oils in asphalts. *Ind. Eng. Chem. Res. Dev.* **1974**, *13*, 65−70.
(42) Eyssautier, J.; Frot, D.; Barré, L. Structure and dynamic properties of colloidal asphaltene aggregates. *Langmuir* **2012**, *28*, 11997−12004.
(43) Erni, P. Deformation modes of complex fluid interfaces. *Soft Matter* **2011**, *7*, 7586−7600.
(44) Gibbs, J. W. *The Collected Works of J. W. Gibbs*; Lonmans: Green, New York, NY, 1931; Vol. *1*.
(45) Le Grand, A.; Petekidis, G. Effects of particle softness on the rheology and yielding of colloidal glasses. *Rheol. Acta* **2008**, *47*, 579−590.
(46) Brown, J. J.; Porter, J. A.; Daghlian, C. P.; Gibson, U. J. Ordered arrays of amphiphilic gold nanoparticles in Langmuir monolayers. *Langmuir* **2001**, *17*, 7966−7969.
(47) Pepicelli, M.; Verwijlen, T.; Tervoort, T. A.; Vermant, J. Characterization and modelling of Langmuir interfaces with finite elasticity. *Soft Matter* **2017**, *13*, 5977−5990.
(48) Kotula, A. P.; Anna, S. L. Insoluble layer deposition and dilatational rheology at a microscale spherical cap interface. *Soft Matter* **2016**, *12*, 7038−7055.
(49) Mahani, H.; Keya, A. L.; Berg, S.; Bartels, W.-B.; Nasralla, R.; Rossen, W. R. Insights into the mechanism of wettability alteration by low-salinity flooding (LSF) in carbonates. *Energy Fuels* **2015**, *29*, 1352−1367.
(50) Chakravarthy, R.; Naik, G. N.; Savalia, A.; Sridharan, U.; Saravanan, C.; Das, A. K.; Gudasi, K. B. Determination of naphthenic acid number in petroleum crude oils and their fractions by mid-Fourier transform infrared spectroscopy. *Energy Fuels* **2016**, *30*, 8579−8586.

https://doi.org/10.1021/acs.langmuir.2c00058
Langmuir 2022, 38, 6523−6530